Radiative heat transfer capability implemented in OpenNCC for conjugate heat transfer applications

Makoto Endo
NASA John H. Glenn Research Center
Cleveland, Ohio

Thermal & Fluids Analysis Workshop
TFAWS 2023
August 21-25, 2023
NASA Goddard Space Flight Center
Greenbelt, MD

Introduction

- Thermal efficiency of gas turbine increases as the temperature and the pressure at the combustor increases.
  - **Materials used inside a combustor must survive a challenging environment.**
  - **Effective placement of effusion holes can lead to overall efficiency improvement.**
- Radiative heat transfer in a gas turbine combustor is particularly interesting:
  - **Less frequently incorporated in CFD analysis but has been reported to be important.**
  - **The cooling air may protect the liners from convection but not necessary from radiation.**
  - **May affect the emission performance.**
- Radiative heat transfer solver has been incorporated in OpenNCC.

After presenting the theory and the strategy of implementation, results of validation cases for gray gas and non-gray gas will be presented.

Governing Equations

Radiative Transfer Equation (RTE) with pseudo time marching term:

$$\frac{\partial I_{i,m}}{\partial t} = -\frac{\partial I_{i,m}}{\partial s_m} + \hat{\kappa}_i \hat{\alpha}_i I_b - \hat{\kappa}_i I_{i,m}$$

a-factor

k-factor

Note:
a-factor and k-factor are placeholders to accommodate different spectral models (currently FSCK and WSGG)

Discrete Ordinate method to transform from "path of light" to cartesian coordinate system:

$$\nabla \cdot \mathbf{q_R} = \sum_{i=1}^{n_s} w_i \hat{\kappa}_i \left(4\pi \hat{\alpha}_i I_b - \sum_{m=1}^{n_c} \left(w_m I_{i,m} \right) \right)$$

:Divergence of radiative heat flux (= -S_R)

$$\mathbf{q_R} \cdot \mathbf{n} = \sum_{i=1}^{n_s} w_i \sum_{m=1}^{n_c} \left(w_m I_{i,m} \cdot \mathbf{n} \right)$$

:Radiative wall heat flux

angular resolution: $1 \leq$ m $\leq n_c$ with angular weight of , w_m

spectral resolution: $1 \leq$ i $\leq n_s$ with spectral weight of , w_i

Implementation procedure

- **For the DO method, T4 quadrature set by Thurgood [9] is used (128 directions in 3D) but other options are available.**

- **The radiation solver and the CFD solver shares the same cell-centered, FVM mesh partitioned by METIS [7]. Non-blocking MPI and noncontiguous collective MPI-IO used for communication.**

- **The WSGG model by Bordbar [5] and FSCK model by Modest [6] has been implemented for testing purposes (not for distribution). Between these two models, the WSGG model has less equations to solve and the evaluation of cell-centered properties is found to be quicker. FSCK can handle larger range of species concentration.**

- **The paper Contains more information:**
  - Boundary conditions
  - Characteristic time scale for the radiation solver
  - Spectral models
  - Numerical methods

- In this problem, we are interested in the accuracy associated with angular and spatial discretization.
- Cubic enclosure filled with gas at uniform temperature.
- All walls are cold and black.
- Mesh is 25x25x25 cells.
- Calculation is performed for three different absorption coefficients, namely, 0.1, 1.0 and 10.0 [1/m].

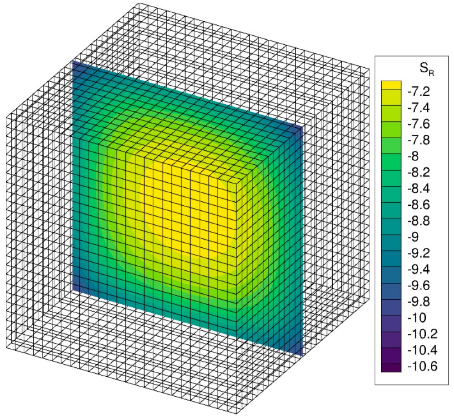

Fig. 1 Uniform mesh used for gray-gas validation (The contour shows the non-dimensional S_R for $\kappa = 1.0$)

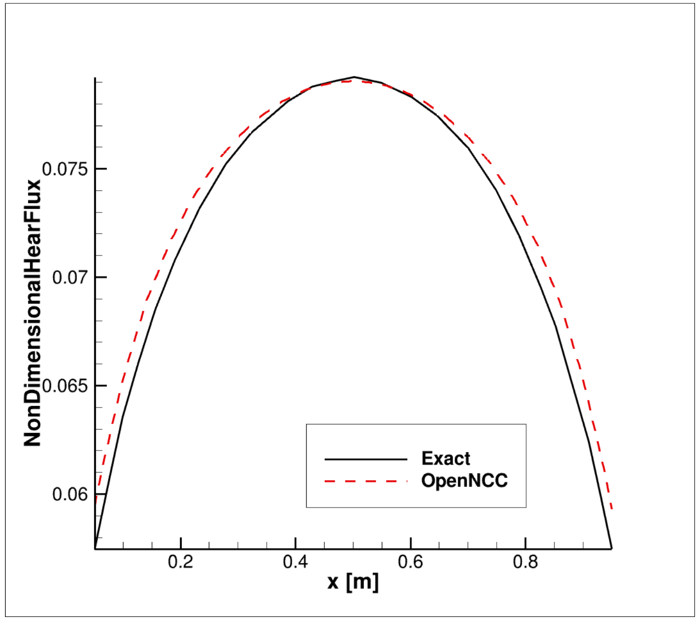

(a) Comparison of wall heat flux: κ=0.1

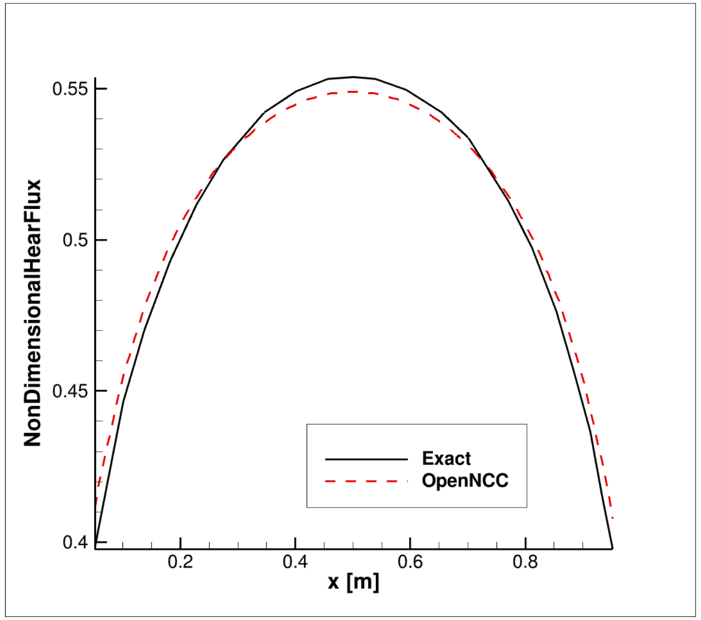

(b) Comparison of wall heat flux: κ=1.0

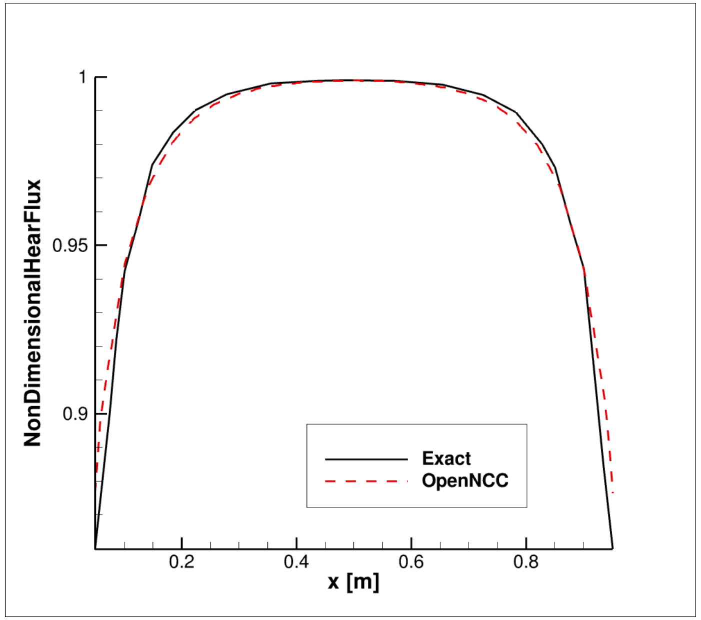

(c) Comparison of wall heat flux: κ=10.0

Non-Gray Gas Validation(1/4)

- **In these problems, we are interested in the accuracy associated with the modeling of participating media.**
- **The geometry is a 2m x 2m x 4m rectangular enclosure at 1atm and the temperature distribution are shown in figure.**
- **All walls are black and at a uniform temperature of 300 K.**
- **The participating species are CO_2 and H_2O with molar concentrations listed in Table 1.**

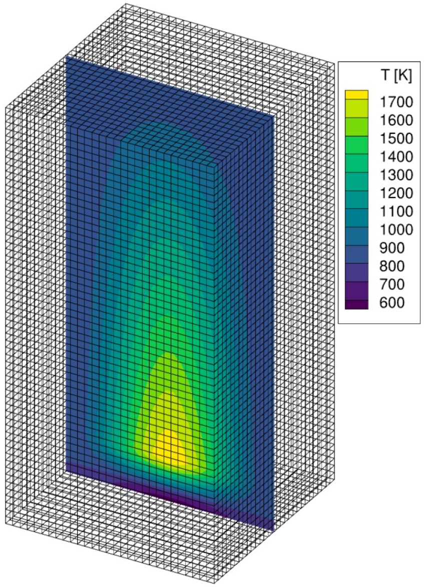

Fig. 3 **Non-gray, uniform mesh, 49,619 cells (29x29x59)**

Table 1 **Species concentration for non-gray test problem**

case number	x_{H_2O}	x_{CO_2}	source
1	0.2	0.1	case 3 of Fraga et al. [12]
2	flame shaped distribution	$x_{H_2O}/2$	case 4 of Fraga et al. [12]
3	0.10	0.85	case 3 of Porter et al. [13]

Table 2 **Computation time comparison using 20CPUs on ivy (units in seconds)**

	case1		case2		case3	
model	FSCK	WSGG	FSCK	WSGG	FSCK	WSGG
run#1	657	74	644	73	698	73
run#2	651	73	639	73	683	73

Non-Gray Gas Validation(2/4)

Table 1 Species concentration for non-gray test problem

case number	x_{H_2O}	x_{CO_2}	source
1	0.2	0.1	case 3 of Fraga et al. [12]
2	flame shaped distribution	$x_{H_2O}/2$	case 4 of Fraga et al. [12]
3	0.10	0.85	case 3 of Porter et al. [13]

- **Both spectral models are capturing the overall trend of radiative source term and wall heat flux.**
- **S_R calculated by the FSCK is slightly higher than the LBL value and the WSGG is lower.**

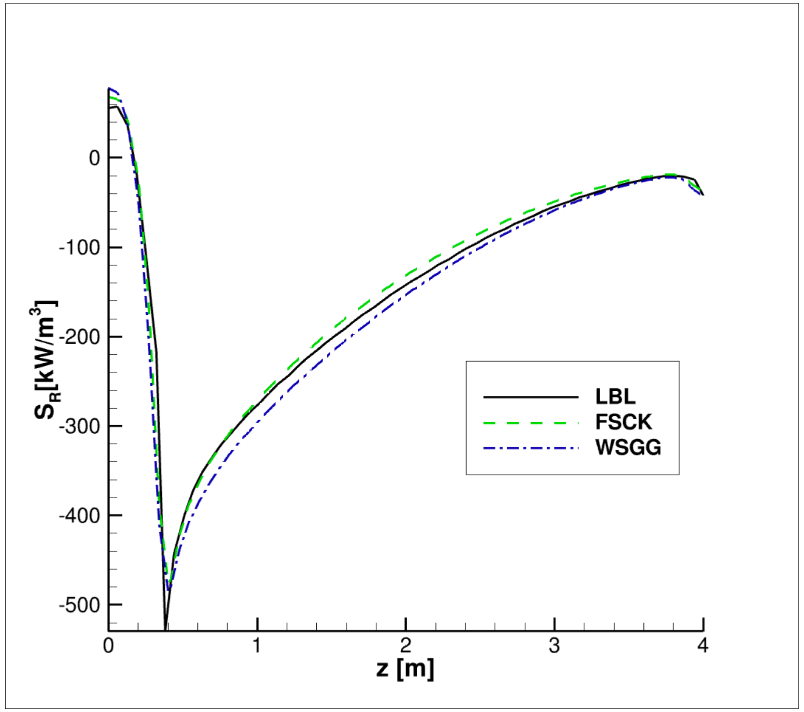

(a) Comparison of radiative source term

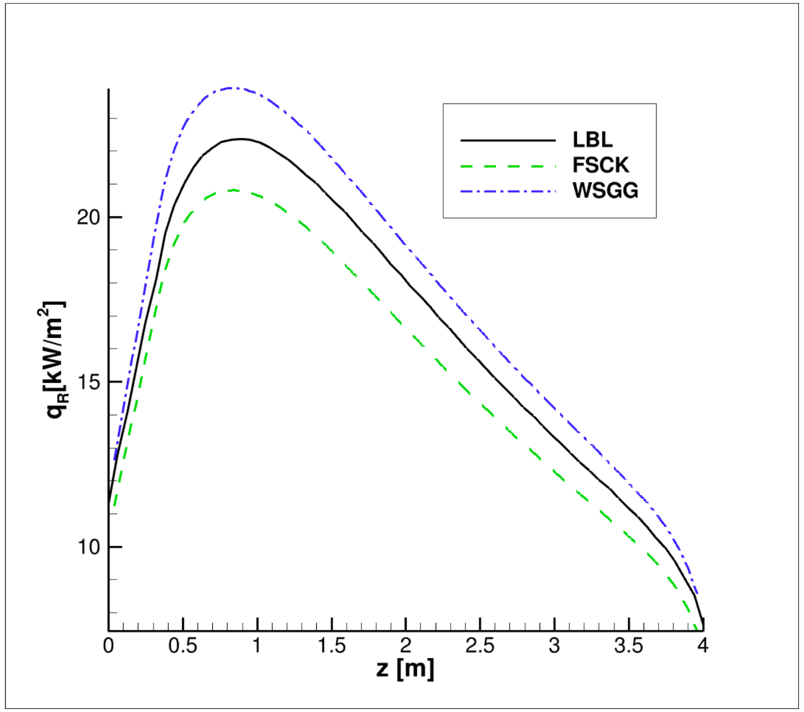

(b) Comparison of wall heat flux

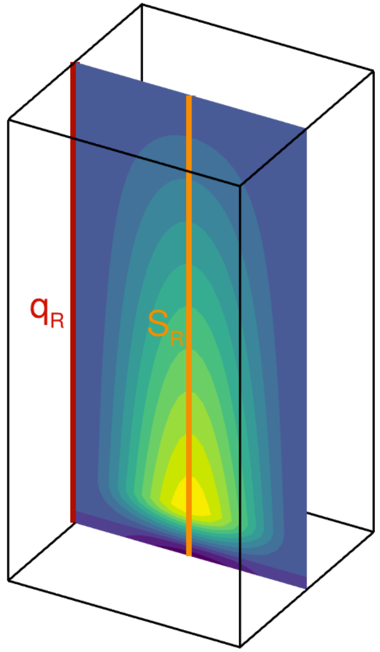

Fig.4 Comparison of case1, LBL data from Fraga et al. [12]

Non-Gray Gas Validation(3/4)

Table 1 Species concentration for non-gray test problem

case number	x_{H_2O}	x_{CO_2}	source
1	0.2	0.1	case 3 of Fraga et al. [12]
2	flame shaped distribution	$x_{H_2O}/2$	case 4 of Fraga et al. [12]
3	0.10	0.85	case 3 of Porter et al. [13]

- **Similar results as case1**
- **q_R calculated by the FSCK is lower than the LBL and the WSGG is higher than the LBL model value.**

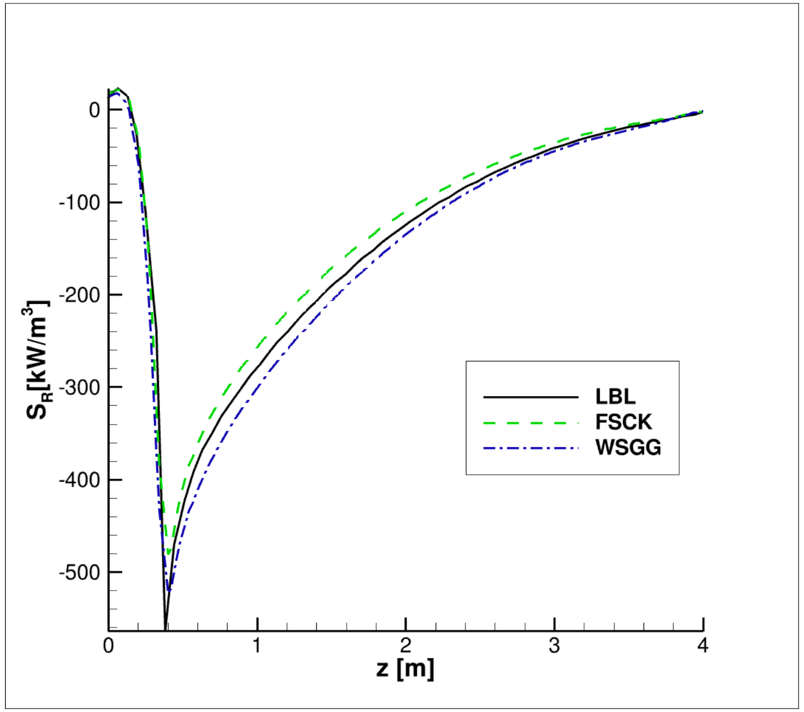

(a) Comparison of radiative source term

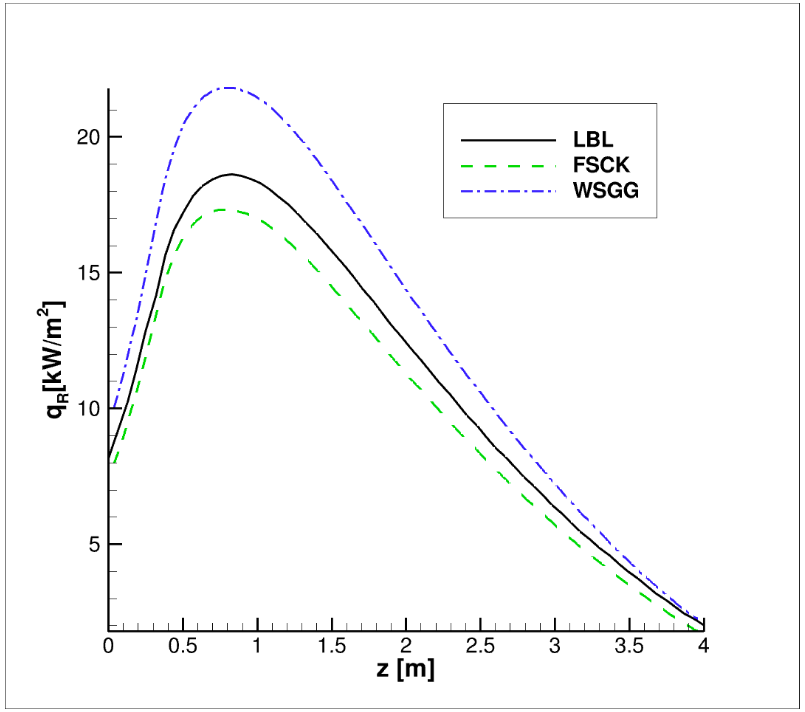

(b) Comparison of wall heat flux

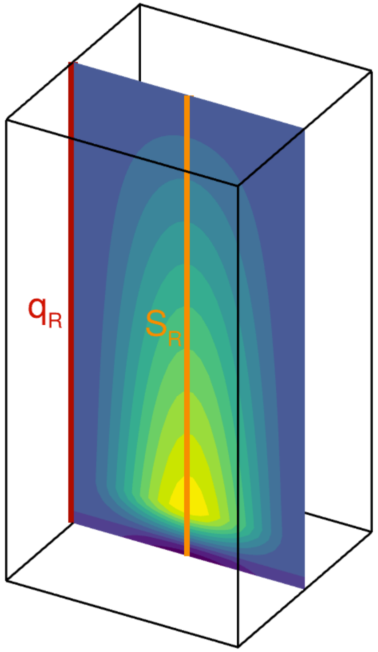

Fig.5 Comparison of case2, LBL data from Fraga et al. [12]

Non-Gray Gas Validation(4/4)

Table 1 Species concentration for non-gray test problem

case number	x_{H_2O}	x_{CO_2}	source
1	0.2	0.1	case 3 of Fraga et al. [12]
2	flame shaped distribution	$x_{H_2O}/2$	case 4 of Fraga et al. [12]
3	0.10	0.85	case 3 of Porter et al. [13]

- **Contrary to the other two cases, case3 has more CO_2 than H_2O.**
- **The relationship between the FSCK model and the WSGG model is being maintained.**

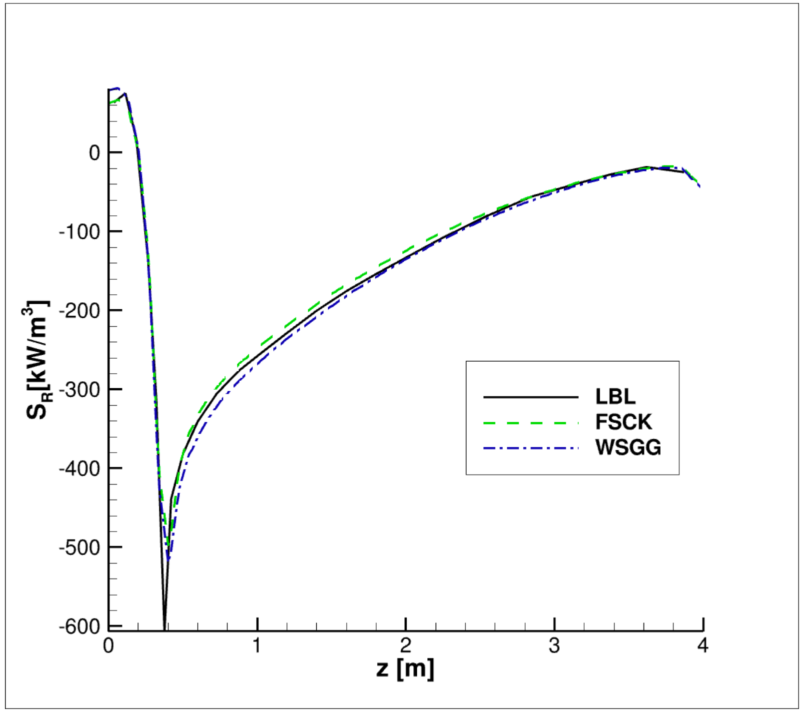

(a) Comparison of radiative source term

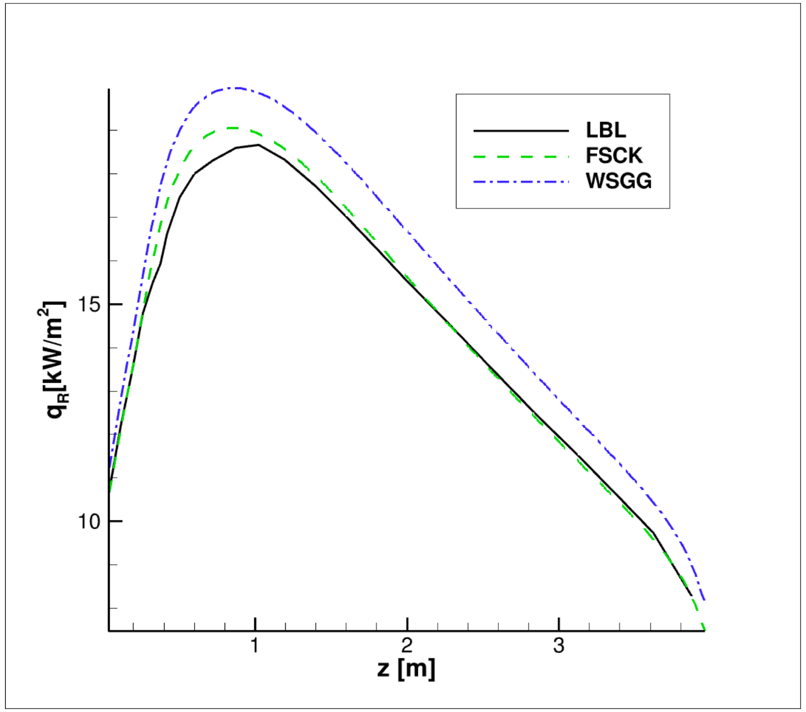

(b) Comparison of wall heat flux

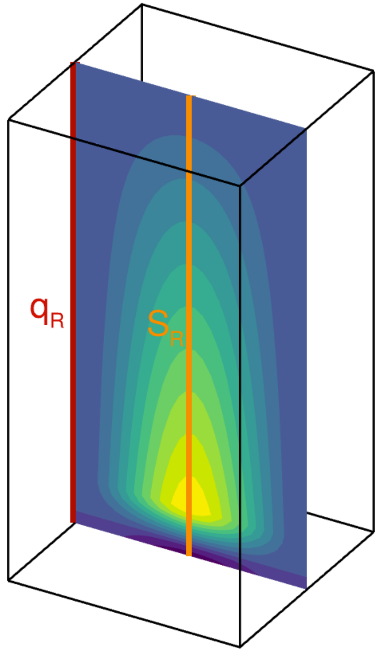

Fig.6 Comparison of case3, LBL data from Porter et al. [12]

Non-Uniform Mesh Validation(1/4)

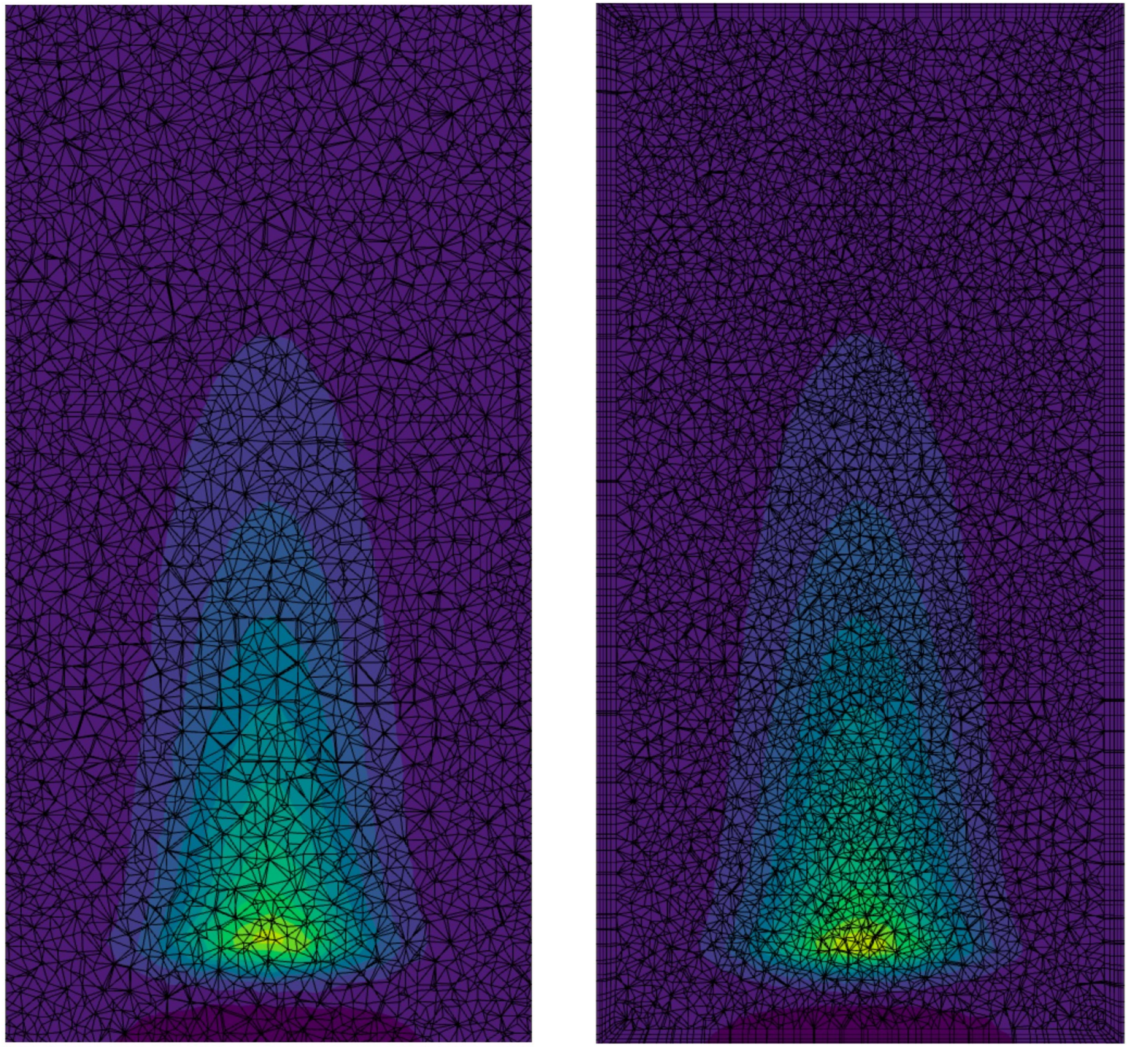

(a) All tetrahederon mesh
(56,773 pts ; 309,722 cells)

(b) Mixed elements mesh
(178,799 pts; 793,297 cells)

Fig.7 mesh distribution compared at the center cut-plane

Table 4 Number of cells in each mesh

Name of the mesh	Number of cells
Uniform-coarse (29x29x59)	49,619
Uniform-dense (59x59x119)	414,239
Non-uniform all tetrahedelon	309,722
Non-uniform mixed elements	793,297

- **The mixed elements mesh has five layers of expanding prisms with minimum wall distance of 1cm.**
- **The mixed elements mesh is denser compared to the all-tetrahedron mesh.**
- **The comparison is performed for both, gray gas problem and non-gray gas problem.**

Non-Uniform Mesh Validation(2/4)

- **Gray gas with uniform (κ, T, T_w)=(1.0, 1000,300)**

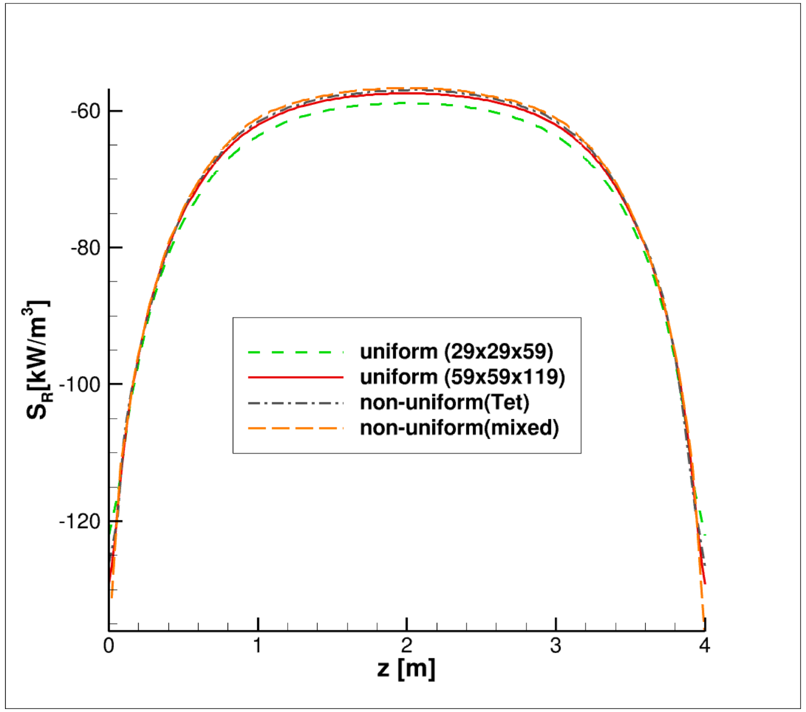

(a) Comparison of radiative source term

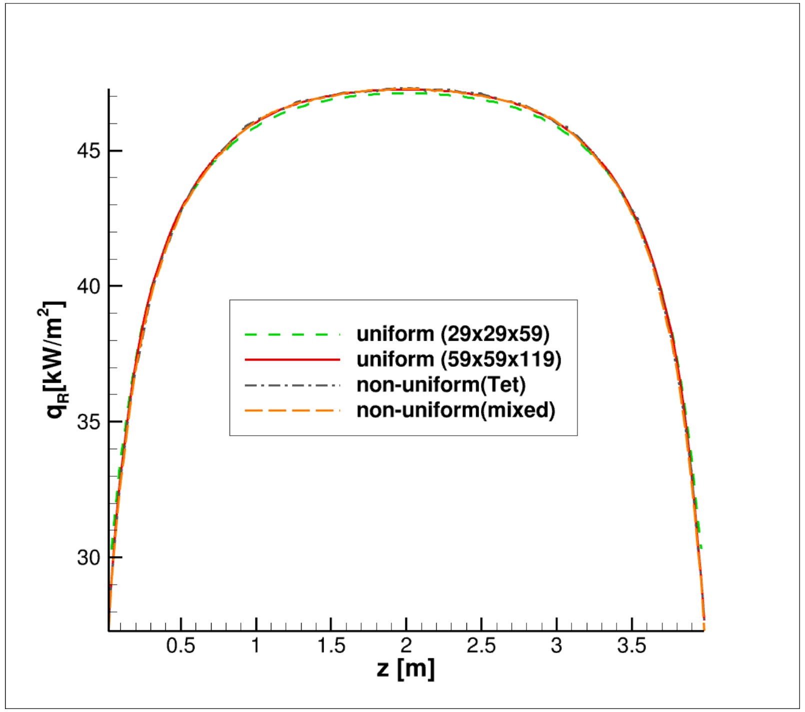

(b) Comparison of wall heat flux

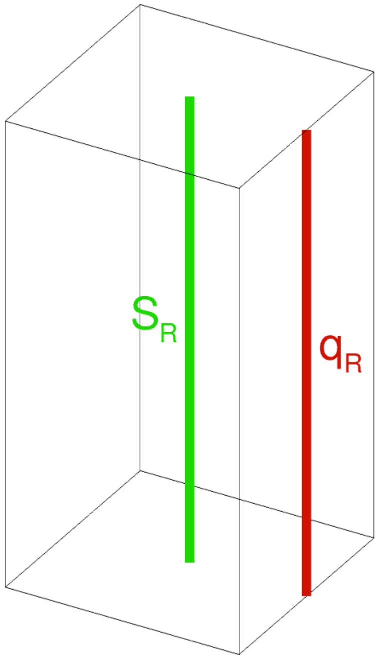

Fig. 8 Comparison of effect of mesh types: gray gas (κ=1.0, T=1000K, T_W=300K)

All four meshes are providing similar results in both, radiative source term and the wall heat flux.
The results of the coarse uniform mesh is slightly away from the other three cases due to the resolution.

Table 1 Species concentration for non-gray test problem

case number	x_{H_2O}	x_{CO_2}	source
1	0.2	0.1	case 3 of Fraga et al. [12]
2	flame shaped distribution	$x_{H_2O}/2$	case 4 of Fraga et al. [12]
3	0.10	0.85	case 3 of Porter et al. [13]

- **Solving case2 with FSCK model.**
- **Oscillation in the wall heat flux gets removed with the mixed elements mesh that has a layer of uniformly distanced cells near the wall.**

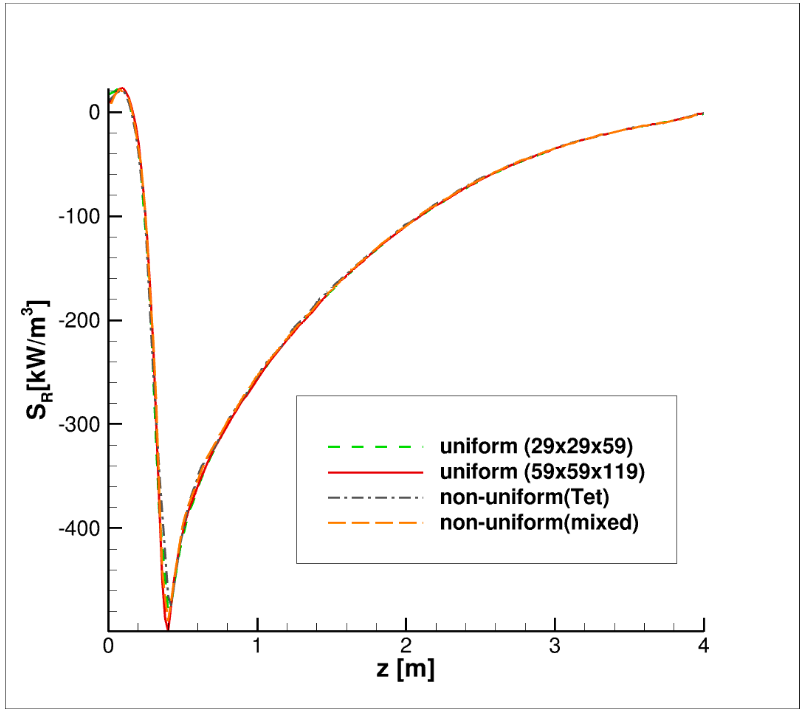

(a) Comparison of radiative source term

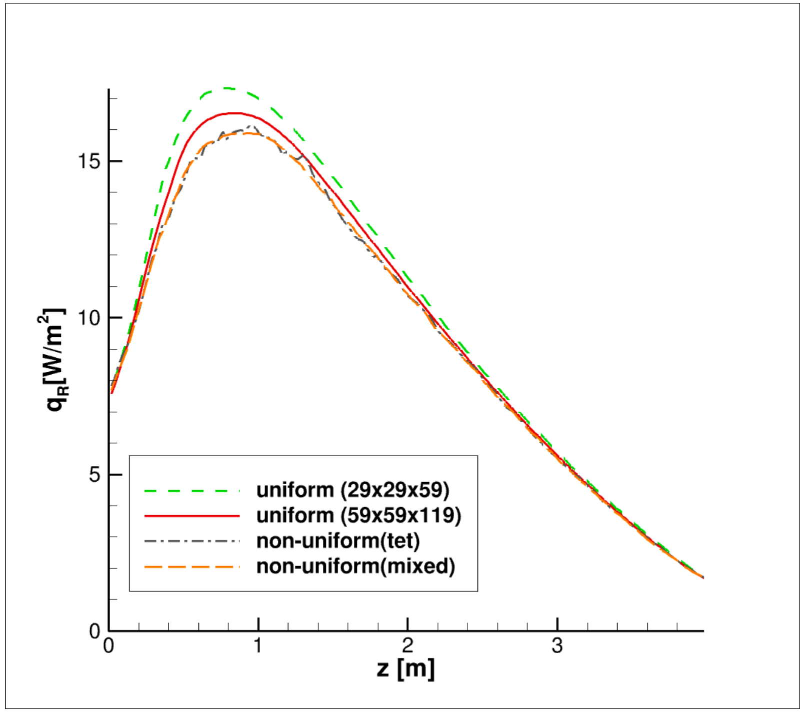

(b) Comparison of wall heat flux

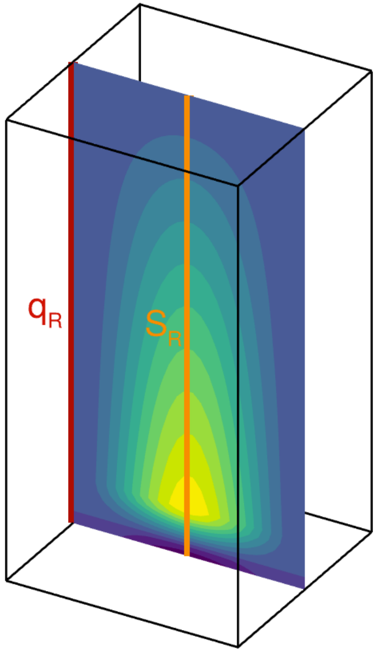

Fig.9 Comparison of effect of mesh types: case2 using FSCK

Non-Uniform Mesh Validation(4/4)

Table 1 Species concentration for non-gray test problem

case number	x_{H_2O}	x_{CO_2}	source
1	0.2	0.1	case 3 of Fraga et al. [12]
2	flame shaped distribution	$x_{H_2O}/2$	case 4 of Fraga et al. [12]
3	0.10	0.85	case 3 of Porter et al. [13]

- **Solving case2 with WSGG model.**
- **Similar trend as FSCK.**
- **Improving the resolution of the uniform mesh makes the wall heat flux values closer to the non-uniform mesh solutions.**

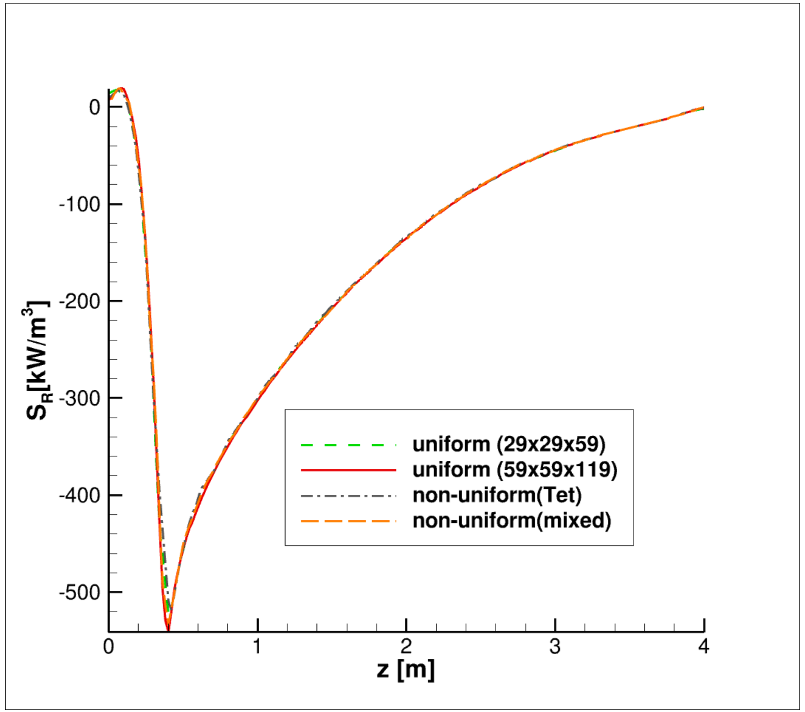

(a) Comparison of radiative source term

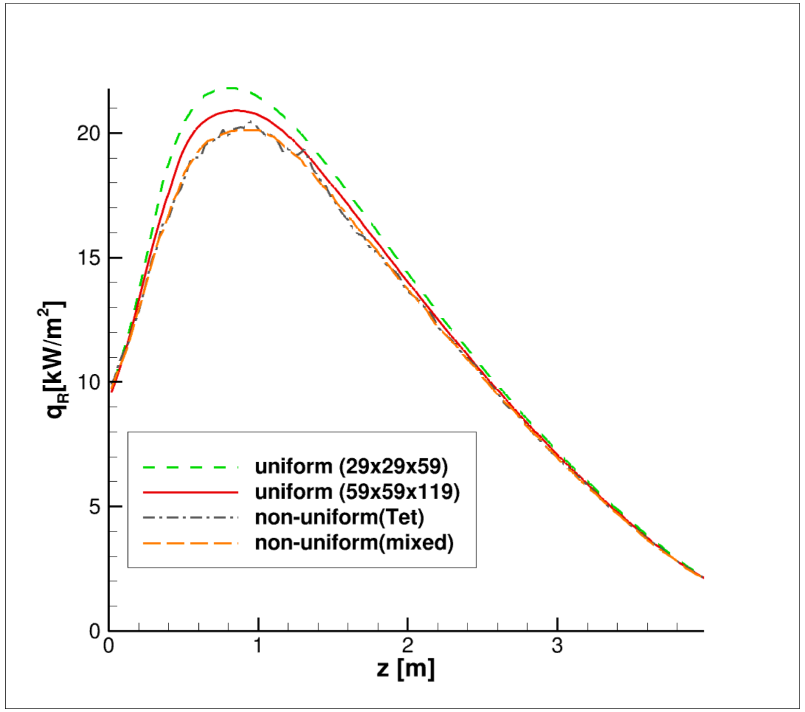

(b) Comparison of wall heat flux

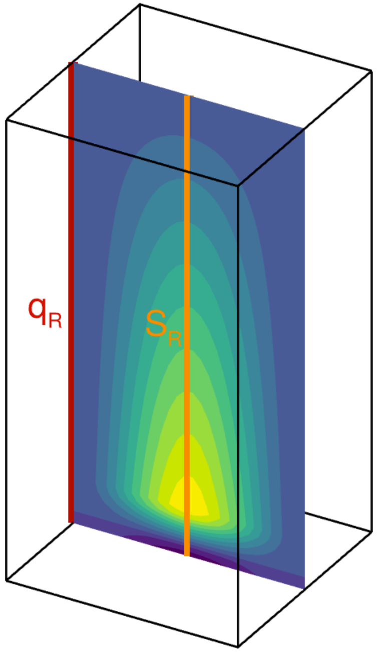

Fig.10 Comparison of effect of mesh types: case2 using WSGG

Summary

- The theory and the implementation of the newly developed radiative heat transfer capability added to OpenNCC has been explained and its performance has been presented through series of validation problems.
- The computed results were in good agreement with the reference solutions for gray-gas and non-gray gas problems.
- The radiation solver performed well when applied to non-uniform (unstructured) mesh.
- This solver is expected to be combined with other capabilities of OpenNCC and applied to a realistic engineering problem.

Acknowledgments

This work was supported by the Transformational Tools and Technologies Project under the NASA Aeronautics Research Mission Directorate.

Resources supporting this work were provided by the NASA High-End Computing (HEC) Program through the NASA Advanced Supercomputing (NAS) Division at Ames Research Center.

References (1/2)

[1] Berger, S., Richard, S., Duchaine, F., Staffelbach, G., and Gicquel, L., "On the sensitivity of a helicopter combustor wall temperature to convective and radiative thermal loads," *Applied Thermal Engineering*, Vol. 103, 2016, pp. 1450–1459. https://doi.org/https://doi.org/10.1016/j.applthermaleng.2016.04.054, URL https://www.sciencedirect.com/science/article/pii/S1359431116305403.

[2] Endo, M., Tacina, K. M., Hicks, Y. R., Capil, T., and Moder, J. P., "Numerical Simulation of Lean Blowout of Alternative Fuels in 7-element Lean Direct Injector," *AIAA Propulsion and Energy 2021 Forum*, American Institute of Aeronautics and Astronautics, 2021. https://doi.org/10.2514/6.2021-3458, URL https://arc.aiaa.org/doi/abs/10.2514/6.2021-3458.

[3] Wey, C. T., "Fuel Sensitivity of Lean Blowout in a RQL Gas Turbine Combustor," *AIAA Propulsion and Energy 2019 Forum*, American Institute of Aeronautics and Astronautics, 2019, p. 170. https://doi.org/10.2514/6.2019-4035, URL https://arc.aiaa.org/doi/abs/10.2514/6.2019-4035.

[4] Ajmani, K., Lee, P., Chang, C. T., and Tacina, K. M., "Pilot Injector Redesign to Reduce N+3 Cycle Emissions For A Gas-Turbine Combustor," *AIAA Propulsion and Energy 2019 Forum*, American Institute of Aeronautics and Astronautics, 2019. https://doi.org/10.2514/6.2019-4371, URL https://arc.aiaa.org/doi/abs/10.2514/6.2019-4371.

[5] Bordbar, H., Coelho, F. R., Fraga, G. C., França, F. H., and Hostikka, S., "Pressure-dependent weighted-sum-of-gray-gases models for heterogeneous CO2-H2O mixtures at sub- and super-atmospheric pressure," *International Journal of Heat and Mass Transfer*, Vol. 173, 2021, p. 121207. https://doi.org/https://doi.org/10.1016/j.ijheatmasstransfer.2021.121207, URL https://www.sciencedirect.com/science/article/pii/S0017931021003100.

[6] Modest, M. F., "Spectral Radiation Calculation Software (SRCS)," provided by M. F. Modest to NASA Glenn Research Center under NASA Grant NNX07AB40A, 2008.

[7] Karypis, G., and Kumar, V., "METIS: A Software Package for Partitioning Unstructured Graphs, Partitioning Meshes, and Computing Fill-Reducing Orderings of Sparse Matrices," Retrieved from the University of Minnesota Digital Conservancy, 1997. URL https://hdl.handle.net/11299/215346.

References (2/2)

[8] Gottlieb, S., and Shu, C.-W., "Total variation diminishing Runge-Kutta schemes," *Mathematics of Computation*, Vol. 67, No. 221, 1998, pp. 73–85.

[9] Thurgood, C., "A critical evaluation of the discrete ordinates method using HEART and Tn quadrature," Ph.D. thesis, Queen's University, Kingston, Canada, 1992.

[10] Kang, S. H., and Song, T.-H., "Finite element formulation of the first- and second-order discrete ordinates equations for radiative heat transfer calculation in three-dimensional participating media," *Journal of Quantitative Spectroscopy and Radiative Transfer*, Vol. 109, No. 11, 2008, pp. 2094–2107. https://doi.org/10.1016/j.jqsrt.2008.02.016.

[11] Liu, F., "Numerical Solutions of Three-Dimensional Non-Grey Gas Radiative Transfer Using the Statistical Narrow-Band Model," *Journal of Heat Transfer*, Vol. 121, No. 1, 1999, pp. 200–203. https://doi.org/10.1115/1.2825944, URL https://doi.org/10.1115/1.2825944.

[12] Fraga, G. C., Bordbar, H., Hostikka, S., and França, F. H. R., "Benchmark Solutions of Three-Dimensional Radiative Transfer in Nongray Media Using Line-by-Line Integration," *Journal of Heat Transfer*, Vol. 142, No. 3, 2020. https://doi.org/10.1115/1.4045666, URL https://doi.org/10.1115/1.4045666, 034501.

[13] Porter, R., Liu, F., Pourkashanian, M., Williams, A., and Smith, D., "Evaluation of solution methods for radiative heat transfer in gaseous oxy-fuel combustion environments," *Journal of Quantitative Spectroscopy and Radiative Transfer*, Vol. 111, No. 14, 2010, pp. 2084–2094. https://doi.org/https://doi.org/10.1016/j.jqsrt.2010.04.028, URL https://www.sciencedirect.com/science/article/pii/S0022407310001652.

[14] "Pleiades Configuration Details," Online, Retrieved Jul21, 2023. URL https://www.nas.nasa.gov/hecc/support/kb/pleiades-configuration-details_77.html.

TFAWS

GSFC · 2023